Mapping the interaction between the hemophore HasA and its outer membrane receptor HasR using CRINEPT-TROSY NMR spectroscopy

ARTICLE *in* JOURNAL OF THE AMERICAN CHEMICAL SOCIETY · FEBRUARY 2009

Impact Factor: 12.11 · DOI: 10.1021/ja804783x · Source: PubMed

Article

Mapping the Interaction between the Hemophore HasA and Its Outer Membrane Receptor HasR Using CRINEPT#TROSY NMR Spectroscopy

Ce#lia Caillet-Saguy, Mario Piccioli, Paola Turano, Nadia Izadi-Pruneyre, Muriel Delepierre, Ivano Bertini, and Anne Lecroisey

J. Am. Chem. Soc., **Article ASAP** • DOI: 10.1021/ja804783x

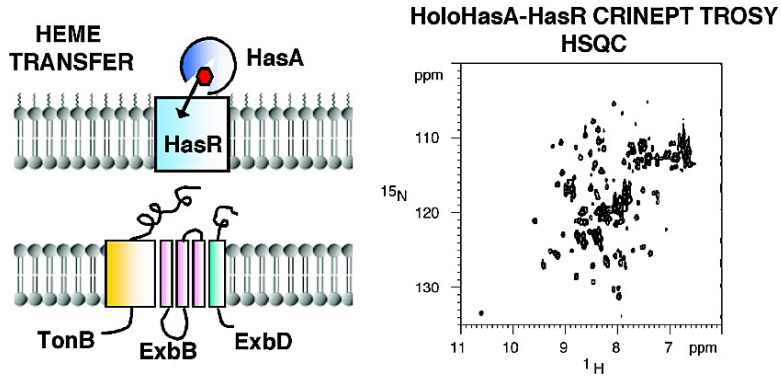

More About This Article

Additional resources and features associated with this article are available within the HTML version:

- Supporting Information
- Access to high resolution figures
- Links to articles and content related to this article
- Copyright permission to reproduce figures and/or text from this article

View the Full Text HTML

J|A|C|S
ARTICLES

Mapping the Interaction between the Hemophore HasA and Its Outer Membrane Receptor HasR Using CRINEPT−TROSY NMR Spectroscopy

Célia Caillet-Saguy,[†] Mario Piccioli,[‡] Paola Turano,[‡] Nadia Izadi-Pruneyre,[†] Muriel Delepierre,[†] Ivano Bertini,[‡] and Anne Lecroisey*[,†]

Unité de RMN des Biomolécules (CNRS URA 2185), Institut Pasteur, Paris, France, and CERM and Department of Chemistry, University of Florence, Sesto Fiorentino, Florence, Italy

Received June 23, 2008; E-mail: alecrois@pasteur.fr

Abstract: The first step of heme acquisition by Gram-negative pathogenic bacteria through the so-called heme acquisition system, Has, requires delivery of the heme from the extracellular hemophore protein HasA to a specific outer membrane receptor, HasR. CRINEPT−TROSY NMR experiments in DPC micelles were here used to obtain information on the intermediate HasA−HasR complex in solution. A stable protein−protein adduct is detected both in the presence and in the absence of heme. Structural information on the complexed form of HasA is obtained from chemical shift mapping and statistical analysis of the spectral fingerprint of the protein NMR spectra obtained under different conditions. This approach shows the following: (i) only three different conformations are possible for HasA in solution: one for the isolated apoprotein, one for the isolated holoprotein, and one for the complexed protein, that is independent of the presence of the heme; (ii) the structure of the hemophore in the complex resembles the open conformation of the apoprotein; (iii) the surface contact area between HasA and HasR is independent of the presence of the heme, involving loop L1, loop L2, and the $\beta2-\beta6$ strands; (iv) upon complex formation the heme group is transferred from holoHasA to HasR.

Introduction

One of the strategies developed by many Gram-negative pathogenic bacteria to acquire iron is the so-called heme acquisition system Has, which relies on the extracellular hemophore protein HasA.[1] This protein, once secreted by bacteria, binds free heme or extracts heme from host hemoproteins such as hemoglobin and delivers it to a specific outer membrane receptor, HasR, which in turn transfers the heme to the periplasmic space.[2,3] The *S. marcescens* hemophore HasA (MW 19 kDa) was the first hemophore to be identified and is the only one structurally characterized.[4,5] The structures of both apo and holo forms have been determined by solution NMR and X-ray crystallography, respectively (Figure 1).[4,5] The protein fold presents a curved antiparallel β-sheet of seven strands on one face and four α-helices on the other face. In holoHasA, the heme is held by two extended loops, L1 (G28-G43) and L2 (Y75-T84). The heme iron(III) ion is coordinated to H32 on loop L1, and Y75 on loop L2. The Y75 Oη forms a tight H-bond with the Nδ1 of a nearby histidine, H83, that stabilizes the tyrosine in a coordinating state.[6,7] In apoHasA, loop L1

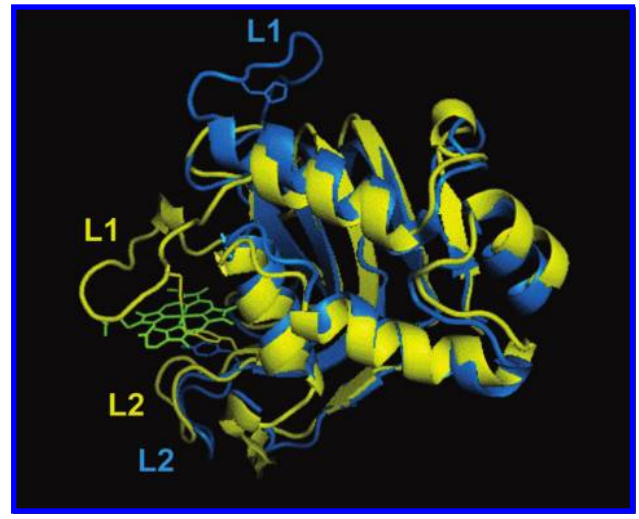

Figure 1. Overlay of the NMR structure of apoHasA in blue (PDB id 1YBJ) and X-ray structure of holoHasA in yellow (PDB id 1B2V). The two axial ligands, H32 on loop L1 and Y75 on loop L2, are shown as lines. Heme in holoHasA is in yellow.

[†] Institut Pasteur.
[‡] University of Florence.

(1) Letoffe, S.; Ghigo, J. M.; Wandersman, C. *Proc. Natl. Acad. Sci. U.S.A.* **1994**, *91*, 9876–80.
(2) Ghigo, J. M.; Letoffe, S.; Wandersman, C. *J. Bacteriol.* **1997**, *179*, 3572–9.
(3) Paquelin, A.; Ghigo, J. M.; Bertin, S.; Wandersman, C. *Mol. Microbiol.* **2001**, *42*, 995–1005.
(4) Arnoux, P.; Haser, R.; Izadi, N.; Lecroisey, A.; Delepierre, M.; Wandersman, C.; Czjzek, M. *Nat. Struct. Biol.* **1999**, *6*, 516–20.
(5) Wolff, N.; Izadi-Pruneyre, N.; Couprie, J.; Habeck, M.; Linge, J.; Rieping, W.; Wandersman, C.; Nilges, M.; Delepierre, M.; Lecroisey, A. *J. Mol. Biol.* **2008**, *376*, 517–25.
(6) Wolff, N.; Deniau, C.; Letoffe, S.; Simenel, C.; Kumar, V.; Stojiljkovic, I.; Wandersman, C.; Delepierre, M.; Lecroisey, A. *Protein Sci.* **2002**, *11*, 757–65.
(7) Caillet-Saguy, C.; Delepierre, M.; Lecroisey, A.; Bertini, I.; Piccioli, M.; Turano, P. *J. Am. Chem. Soc.* **2006**, *128*, 150–8.

undergoes important conformational changes. It is displaced up to 30 Å with respect to its position in holoHasA, protruding toward the exterior of the protein which thus assumes an open conformation (Figure 1). The receptor HasR is a 95 kDa protein that belongs to the TonB dependent receptor family. It shows the β-barrel structure typical of these receptors.[8,9]

Both holo and apoHasA bind tightly to HasR ($K_a > 10^9\ M^{-1}$) with a 1/1 stoichiometry,[10] and the complex formation is irreversible in absence of both energy source and of heme.[10] HasA binds heme with a high affinity ($K_a = 5.5 \times 10^{10}\ M^{-1}$),[11,12] while HasR has a lower affinity for the heme than HasA (K_a of $5 \times 10^{-6}\ M^{-1}$). In a previous work, some of us have shown that heme is transferred from its binding site on HasA to its binding site on HasR upon complex formation.[10] The transfer is driven by a protein−protein interaction and does not require energy. For the biological function, the heme should be then transferred from the receptor into the periplasm and the apo hemophore should be released from binding to the receptor. These two processes require energy which in vivo is provided by an inner membrane complex of three proteins: HasB, ExbB, and ExbD,[13] HasB being an analogue of TonB specific for HasR.[3]

Understanding at the atomic level the mechanism of heme transfer between HasA and HasR represents a contribution to unravel the factors governing the trafficking of metal cofactors in biology. In order to learn about this process in solution, the interaction between the heme-loaded and heme-free hemophore and the HasR receptor solubilized in DPC micelles was studied. CRINEPT−TROSY NMR spectroscopy provided structural information on the intermediate HasA−HasR complexes and on the first step of heme internalization. The proposed NMR approach is based on the use of the $^1H-^{15}N$ HSQC patterns as fingerprint of the possible HasA conformations: the "open" conformation of the apoHasA and the "closed" conformation of the holoprotein. To circumvent the lack of a complete assignment of both holo and apo complexes, a spectral profiling analysis, that relies on the calculation of a distance matrix, was used to monitor HasA conformations in both free and complexed states. The obtained results show that HasA possesses three spectral signatures in solution that correspond to its possible conformations i.e., the open structure of isolated apoHasA, the closed structure of isolated holoHasA, and a unique structure for the HasA−HasR complex, which is independent of the presence of the heme. The latter closely resembles that of the apoprotein.

Materials and Methods

Expression and Purification of HasA Hemophore from *Serratia marcescens*. Wild-type HasA was expressed in *E. coli* strain POP3 transformed with plasmid pSYC34 (pAM238).[1] Uniformly $^{15}N/^2H$ labeled protein was produced in a 1 L fermentor at 303 K and in 100% D_2O M9 minimal medium containing $^{15}NH_4Cl$ and ^2H-glycerol as the sole nitrogen and carbon sources. In order to adapt *E. coli* cells to a fully deuterium-containing medium, a six-step procedure was adopted. The first preculture was performed in 100% H_2O M9 minimal medium. Four consecutive precultures were then performed in M9 medium prepared with 100% D_2O, followed by the 1 L culture. For all precultures, growth was stopped at $OD_{600nm} \approx 0.7$, an aliquot of the culture medium was centrifuged, and the pellet was used to inoculate the subsequent culture at $OD_{600nm} \approx 0.1$. The 1 L culture was stopped at $OD_{600nm} = 1.6$. Yield was 50 mg of $^{15}N/^2H$ HasA. Purification of $^{15}N/^2H$ HasA and cleavage of the C-terminal residues (A180−A188) by the *S. marcescens* protease PrtSM were performed as described previously,[11,14] except for the buffer which was changed to 20 mM phosphate buffer pH 7. Cleavage and purity of the perdeuterated protein were checked by SDS-PAGE and MALDI-TOF mass spectrometry (CIPHERGEN). Percentage of deuteration was estimated to 99.7 ± 0.1%.

Preparation of holoHasA was performed by addition of an excess of freshly prepared hemin as previously described.[7] The excess of heme was eliminated by size exclusion chromatography to obtain 100% heme-loaded protein, as monitored by the absence of apoprotein resonances in the $^1H-^{15}N$ HSQC spectra. Apo and holoHasA samples were dialyzed against 20 mM NH_4HCO_3 and freeze-dried.

Expression and Purification of HasR Receptor from *Serratia marcescens*. Receptor HasR was expressed in *E. coli* strain Popc4420 (a OmpF− OmpC− LamB− derivative of MC4100) transformed with plasmid pFR2 (a pBAD24 derivative) under arabinose control. Cells were grown at 30 °C in M9 minimal medium containing 0.4% glycerol, 0.2% casamino acids, 50 μM $FeSO_4$, and 50 μM sodium citrate in a 300 L fermentor. Arabinose (40 mg/liter) was added when the culture reached an OD_{600nm} of 0.7. The cells were harvested after 3 h of induction.[10]

HasR was partially purified from crude membrane preparations obtained after French press treatment. Membranes from 50 g of wet treated cells were suspended and solubilized as previously described,[10] using successively 1%, 2%, and 2.5% ZW3-14 (n-tetradecyl-*N*,*N*-dimethyl-3-ammonio-1-propanesulfonate; Calbiochem). The pooled supernatants from the second and third solubilization were loaded on a 20 mL Q-Sepharose fast-flow column (Amersham Biosciences) equilibrated with 100 mM Tris-HCl at pH 7.5, 0.08% ZW3-14, 10 mM EDTA, and extensively washed with the same buffer (flow-rate 1.6 mL/min; 3 mL fractions). The bound proteins were eluted with a 140 mL linear gradient of 0−1 M NaCl. The fractions containing the receptor were identified by SDS-PAGE and pooled. The pool was concentrated on a 100 kDa cutoff Amicon centriflow filter, and the receptor was purified by size exclusion chromatography on a superdex 200 column (60 × 2.6 cm; Amersham Biosciences) in 100 mM Tris-HCl at pH 7.5, 0.08% ZW3-14. Concentration of purified HasR was estimated using the ε_{278nm} value of 140 000 $M^{-1}cm^{-1}$ [10]. The typical yield was about 10 mg of purified HasR from 10 g of wet cells.

Preparation of the HasA−HasR Complexes. The apoHasA−HasR and holoHasA−HasR complexes were reconstituted in vitro to enable specific $^2H/^{15}N$ labeling of HasA in the complexes. An excess of freeze-dried apo or holoHasA (110% mol/mol) was added to a purified HasR solution, 1.3×10^{-5} M in 100 mM Tris pH 7.5, 0.08% ZW3-14. After 3 h incubation at 4 °C, the solution was loaded on the 20 mL Q sepharose column as above to eliminate the excess of HasA. Uncomplexed HasA was eluted at 0.39 M NaCl and both complexes at 0.72 M NaCl. Complexes were then extensively washed with 100 mM Tris-HCl at pH 7.5, 0.08% ZW3-

(8) Barjon, C.; Wecker, K.; Izadi-Pruneyre, N.; Delepelaire, P. *J. Bacteriol.* **2007**, *189*, 5379–82.
(9) After submission of the present paper, a structure of HasR bound to HasA has been solved at 2.7 Å resolution, which confirms the overall HasR folding proposed on the basis of the homology modeling.
(10) Izadi-Pruneyre, N.; Huche, F.; Lukat-Rodgers, G. S.; Lecroisey, A.; Gilli, R.; Rodgers, K. R.; Wandersman, C.; Delepelaire, P. *J. Biol. Chem.* **2006**, *281*, 25541–25550.
(11) Izadi, N.; Henry, Y.; Haladjian, J.; Goldberg, M. E.; Wandersman, C.; Delepierre, M.; Lecroisey, A. *Biochemistry* **1997**, *36*, 7050–7.
(12) Deniau, C.; Gilli, R.; Izadi-Pruneyre, N.; Letoffe, S.; Delepierre, M.; Wandersman, C.; Briand, C.; Lecroisey, A. *Biochemistry* **2003**, *42*, 10627–33.
(13) Letoffe, S.; Delepelaire, P.; Wandersman, C. *J. Bacteriol.* **2004**, *186*, 4067–74.
(14) Izadi-Pruneyre, N.; Wolff, N.; Redeker, V.; Wandersman, C.; Delepierre, M.; Lecroisey, A. *Eur. J. Biochem.* **1999**, *261*, 562–8.

14 on a 100 kDa cutoff amicon centriflow filter, and concentrated to about 0.1 mM.

Preparation of the NMR Samples. Different surfactants were tested by NMR. Assays were carried out on the apoHasA−HasR complex in the presence of ZW3-14 at different concentrations (0.02%, 0.08%, and 1%), 5 mM ^{2}H DPC (dodecyl phosphocholine), 5 mM ^{2}H SDS (sodium dodecyl sulfate), 5 mM LPPG (lyso 1-palmitoyl phosphatidylglycerol), and amphipol A8-35 (gift of J.-L. Popot) in a 4:1 wt/wt excess.[15] Surfactant exchange was performed on amicon 100 kDa centriflow filter as described below. Flip-back 1D proton spectra of the various complexes were recorded at 303 K on a Varian 600 MHz spectrometer equipped with a cryoprobe and compared. ^{2}H DPC which gave the best signal-to-noise ratio and the lowest line broadening was therefore selected. Preparation of the apoHasA−HasR and holoHasA−HasR NMR samples was performed by washing complexes successively with 5 × 1 mL of 30 mM ^{2}H DPC and 6 × 1 mL of 5 mM ^{2}H DPC 20 mM phosphate buffer pH 7 on amicon 100 kDa centriflow filter. Final concentration of the complexes was 320−360 μM.

Free apo and holoHasA NMR samples were obtained by suspending about 2 mg of lyophilized protein in 250 μL of 5 mM ^{2}H DPC 20 mM phosphate buffer pH 7.

NMR Spectroscopy. NMR experiments were carried out at 303 K on a Bruker 900 MHz spectrometer equipped with a TCI cryoprobe. ^{1}H−^{15}N transverse relaxation optimized spectroscopy (TROSY)−heteronuclear single quantum correlation (HSQC) experiments[16] were performed with eight transients per increment and a time domain data size of 1024 × 256 complex points. 2D ^{1}H−^{15}N cross relaxation-enhanced polarization transfer (CRINEPT)−TROSY[17] were performed with transfer periods of 2−3 ms which provided optimal efficiency for the HasA−HasR−DPC complexes. Typical acquisition were done with 1024 scans for each FID for a matrix of 1024 × 200 complex points. Spectra were processed using xwinnmr software package (Bruker) and analyzed using Xeasy (ETH, Zurich). NMR samples contained 15% D_2O, 5 mM ^{2}H DPC, and 20 mM phosphate buffer pH 7.

^{13}C direct-detected NMR experiments[18] were performed on a Bruker Avance 700 MHz spectrometer equipped with a cryogenically cooled probe optimized for the observation of ^{13}C frequencies. ^{13}C−^{13}C NOESY[19] were performed over a 200 ppm spectral window, using mixing times and relaxation delays of 0.6 and 1.3 s, respectively. From 832 to 1440 transients were collected each fid. The data point matrix ranged from 2048 × 230 to 2048 × 295. The overall experimental time for each of the NOESY experiments used in this work was about 7 days.

Chemical Shift Mapping. To express changes in the chemical shifts of the individual amide pairs, the chemical shift change (in ppm) was defined as:[20,21]

$$\Delta\delta_{tot} = ((\Delta\delta_{HN})^2 + (0.16\Delta\delta_N)^2)^{1/2} \quad (1)$$

where $\Delta\delta_{HN/N}$ is the difference of chemical shift of the amide ^{1}H or ^{15}N nuclei, respectively, between two HasA forms and 0.16 is the weight factor of nucleus N (ratio of the average variances of the proton and amide nitrogen chemical shifts observed for the 20 common amino acid residues in proteins deposited in the BioMagResBank (URL http://www.bmrb.wisc.edu)).

Statistical Analysis. Statistical analysis of the ^{1}H−^{15}N NMR maps recorded in DPC micelles for the isolated and complexed hemophore was applied to quantify the distance in the spectral profiles of the four HasA forms relevant for the present paper, i.e., apoHasA, holoHasA, apoHasA−HasR, holoHasA−HasR. The four spectra to be compared were processed with the same apodization function and same number of points in each dimensions. The obtained 2D maps were first segmented into integrated spectral regions of fixed dimensions (0.02 ppm bins in the ^{1}H dimension and 0.50 ppm bins in the ^{15}N dimension) with the AMIX viewer software and then normalized in terms of signal intensity. While in the ^{15}N direction the acquired spectral width was used, in the ^{1}H NMR dimension the analysis was limited to the 6.4−11.0 ppm chemical shift region, to remove possible effects of variations in the suppression of the water resonances. In any case, no signals are present outside the analyzed spectral regions. The distance matrix was then calculated using Euclidean distances between all the four reduced spectra (treated as vectors) and then divided by the maximum value in order to obtain values ranging between 0 and 1. All calculations were done using the "R" statistical environment.[22]

Results

CRINEPT Experiments in DPC Micelles. The ^{1}H−^{15}N TROSY spectra of (^{2}H,^{15}N) of apo and holo HasA in aqueous solution are here reported (Figures 2A and 2B) for the first time; they are substantially identical to those of the (^{1}H,^{15}N) proteins, indicating that 99% deuteration of the protein neither affects the protein structure nor causes changes due to isotopic effects for backbone amides. The HSQC fingerprints of free (^{2}H,^{15}N) apo and holoHasA in aqueous solution are maintained for the two perdeuterated protein forms in DPC micelles (Figures 2C,D vs 2A,B, and superimposition in 2E and 2F), permitting an easy transfer of assignments between the two media. The assignments in DPC micelles are reported in Table S1, Supporting Information.

The complexes between HasA and HasR in DPC micelles were studied in a 1:1 ratio. HasR was in the unlabeled form while HasA was ^{2}H,^{15}N-labeled, as extensive deuteration (in our case up to 99.7%) is useful to reduce the dipolar couplings among protons and therefore the ^{1}H line widths. The large size of the complex (114 kDa) embedded in micelles and the viscosity of the DPC solution, with the consequent slow rotational correlation time, made the ^{1}H NMR signals difficult to detect. As a matter of fact, the ^{1}H−^{15}N TROSY maps of (^{2}H,^{15}N) HasA in the apoHasA−HasR and holoHasA−HasR complexes (data not shown) measured on a 900 MHz spectrometer equipped with a cryoprobe failed to provide any signals beside the five C-terminal residues of the protein. Indeed these residues belong to a mobile tail and therefore are characterized by correlation times shorter than the overall tumbling.

CRINEPT−TROSY is an NMR experiment designed to provide ^{1}H−^{15}N correlations in soluble proteins complexes in the 150 kDa to 1 MDa molecular weight range[17,23] and was used here for the first time to characterize a large protein complex in DPC micelles. The build-up of the CRINEPT efficiency as a function of the transfer delay provided an estimate of the apparent molecular weight for the HasA−HasR complexes in DPC micelles of the order of 150 ± 20 kDa. This

(15) Zoonens, M.; Catoire, L. J.; Giusti, F.; Popot, J. L. *Proc. Natl. Acad. Sci. U.S.A.* **2005**, *102*, 8893–8.
(16) Pervushin, K.; Riek, R.; Wider, G.; Wuthrich, K. *Proc. Natl. Acad. Sci. U.S.A.* **1997**, *94*, 12366–71.
(17) Riek, R.; Wider, G.; Pervushin, K.; Wuthrich, K. *Proc. Natl. Acad. Sci. U.S.A.* **1999**, *96*, 4918–23.
(18) Bermel, W.; Bertini, I.; Felli, I.; Piccioli, M.; Pieratelli, R. *Prog. Nucl. Magn. Reson. Spectrosc.* **2006**, *48*, 25–45.
(19) Matzapetakis, M.; Turano, P.; Theil, E.; Bertini, I. *J. Biomol. NMR* **2007**, *38*, 237–242.
(20) Gsponer, J.; Hopearuoho, H.; Whittaker, S. B.; Spence, G. R.; Moore, G. R.; Paci, E.; Radford, S. E.; Vendruscolo, M. *Proc. Natl. Acad. Sci. U.S.A.* **2006**, *103*, 99–104.
(21) Ayed, A.; Mulder, F. A.; Yi, G. S.; Lu, Y.; Kay, L. E.; Arrowsmith, C. H. *Nat. Struct. Biol.* **2001**, *8*, 756–60.
(22) Ihaka, R.; Gentleman, R. *J. Comput. Stat. Graph.* **1996**, *5*, 299–314.
(23) Riek, R.; Pervushin, K.; Wuthrich, K. *Trends Biochem. Sci.* **2000**, *25*, 462–8.

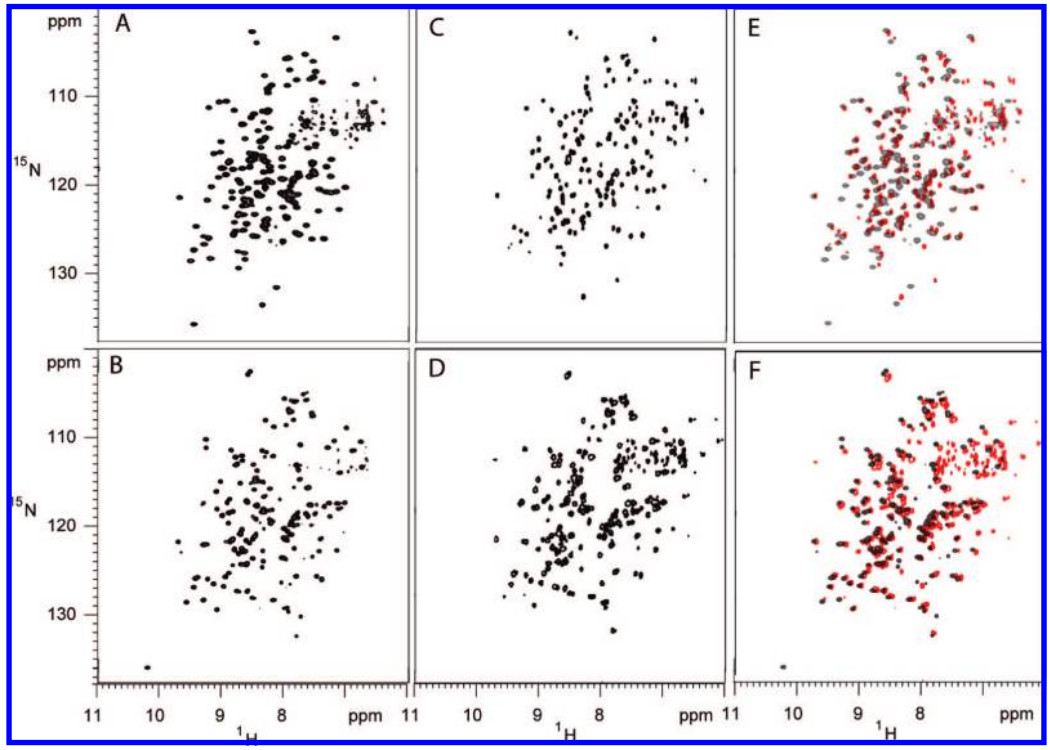

Figure 2. Comparison of the NMR spectra obtained for (^{2}H, ^{15}N) apoHasA and holoHasA under different experimental conditions: 500 MHz TROSY spectra of (A) 1.2 mM apoHasA and (B) 1 mM holoHasA, both in 20 mM phosphate buffer pH 7; 900 MHz TROSY spectra of (C) 0.4 mM apoHasA and (D) 0.4 mM holoHasA, both in 5 mM DPC and 20 mM phosphate buffer pH 7; (E) superimposition of the apoHasA spectra reported in panels A (black) and C (red) and (F) superimposition of the holoHasA spectra reported in panels B (black) and D (red).

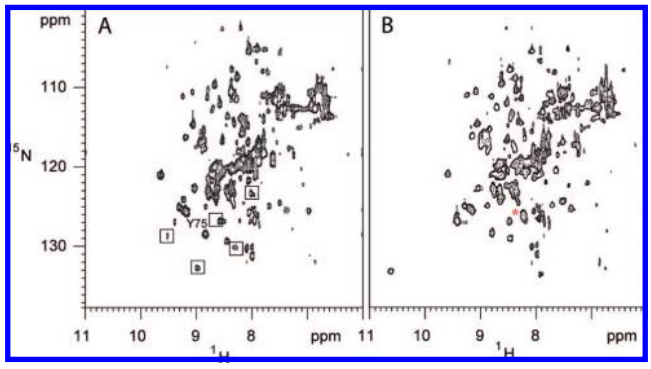

Figure 3. CRINEPT−TROSY spectra of (A) apoHasA−HasR and (B) holo HasA−HasR acquired at 900 MHz, in 5 mM DPC and 20 mM phosphate buffer pH 7. Protein concentrations were 320 μM for apoHasA−HasR and 360 μM for holoHasA−HasR. Boxed peaks in panel A are not present in the spectrum of holoHasA−HasR. A possible candidate peak for Tyr75 in panel B is labeled with a red star.

figure is larger than the sum of the molecular weights of HasA and HasR and is consistent with a slowing down of the tumbling time of the 1:1 protein complexes due to their interaction with DPC micelles. Although the lines were very broad, as observed in Figures 3A and 3B, still 50% of the resonances could be assigned on the basis of chemical shift similarity to the isolated systems, as detailed below. The obtained assignments are listed in Table 1.

The apoHasA−HasR Complex. Binding of HasA to the receptor gives rise to a stable complex which implies specific protein−protein interactions and change in HasA environment due to a closer interaction with the micelle embedding the receptor. The superimposition of apoHasA and apoHasA−HasR complex spectra is shown in Figure 4A.

The chemical shift perturbation to be considered as a threshold level indicative of the protein−protein interaction is larger than values in water solutions. Chemical shift changes in apoHasA spectra upon complex formation provided insights on the regions involved in the interaction with HasR. Two types of signals were useful for the analysis of the chemical shift mapping (Table S2): (1) signals experiencing minimal chemical shift changes (<0.25 ppm), if any, and therefore belonging to regions of HasA that are not affected by the presence of the receptor; (2) signals that undoubtedly disappear from their original well-resolved position in the free apoHasA spectrum upon complex formation and are therefore severely affected when binding to the receptor (either due to large chemical shift changes or to severe line broadening effects caused by a slowing down of exchange rate with the solvent). Residues corresponding to class 1 are reported in gray in Figure 5A, while residues of class 2 are reported in red. Residues whose behavior could not be safely defined, mainly because they fall in crowded spectral regions, are reported in blue. The latter are unsound for the analysis and were not used to map the interaction. Twenty-seven residues, colored in red in Figures 5A and 5B, correspond to signals of class 2 and provide a picture of the contact surface of bound apoHasA. They are residues: W23, G28, D29, V30, H32, V37, D39, G47, L50, G52, A56, A61, N62, A69, N72, L77, N79, A82, H83, L85, Y86, D96, S104, S107, Q109, Q124, and D129. As apparent from Figure 5A, the contact surface is not limited to the two regions of the β face S51−T60 and G95−S107, proposed by site-directed mutagenesis to be relevant for the interaction,[24] but involves a broader area of the protein. Residues of class 2 are all clustered around the heme binding pocket with

(24) Letoffe, S.; Debarbieux, L.; Izadi, N.; Delepelaire, P.; Wandersman, C. *Mol. Microbiol.* **2003**, *50*, 77–88.

Table 1. ^{1}H and ^{15}N NMR Chemical Shift Values (ppm) for apoHasA−HasR and holoHasA−HasR Complexes in 20 mM Phosphate, pH 7, and 5 mM 2H DPC at 303 K

	apoHasA−HasR		holoHasA−HasR			apoHasA−HasR		holoHasA−HasR	
res	N	HN	N	HN	res	N	HN	N	HN
3	123.77	8.64	123.95	8.63	91	111.98	8.52	111.65	8.44
4	121.11	7.93	121.22	7.94	94	121.40	8.79	121.08	8.80
5	113.97	8.32	114.20	8.30	95	108.73	8.25	108.97	8.36
6	122.56	8.44	122.77	8.43	98	125.33	8.41	125.30	8.41
7	118.62	7.79	118.58	7.79	99	120.31	8.79	120.15	8.79
9	122.34	8.71	122.25	8.70	106	121.04	9.61	121.04	9.57
10	119.95	8.66	119.98	8.66	110	120.32	8.33	119.89	8.36
12	106.76	7.90	106.80	7.90	112	123.53	8.76	123.68	8.73
13	102.59	8.52	102.64	8.52	114	117.72	8.83	117.66	8.83
14	123.50	8.31	123.52	8.31	116	111.31	8.79	111.25	8.79
15	114.68	9.04	114.75	9.06	117	107.98	7.78	107.95	7.76
16	122.47	7.38	122.50	7.40	118	117.44	8.99	117.37	8.98
17	115.38	8.84	115.35	8.81	119	112.78	8.69	112.59	8.70
20	119.06	8.47	118.98	8.46	120	117.57	7.32	117.45	7.31
21	105.10	7.87	104.72	7.76	122	116.18	9.16	116.27	9.13
22	124.46	7.48	124.46	7.50	126	113.57	7.24	113.55	7.24
27	123.06	8.77	122.96	8.78	127	105.43	8.04	105.57	8.06
35	114.06	8.83	113.44	8.86	130	108.12	7.61	108.14	7.66
38	119.07	8.75	119.16	8.75	131	123.72	8.58	124.01	8.56
41	120.23	8.04	nd[a]	nd[a]	133	120.36	7.81	120.85	7.81
44	107.74	8.34	107.84	8.46	134	114.56	8.31	114.44	8.31
45	118.87	8.58	118.00	8.56	135	118.28	8.65	118.22	8.67
53	112.89	8.31	113.42	8.31	136	119.00	8.14	119.14	8.28
54	118.21	8.04	118.07	8.04	138	107.11	7.51	107.10	7.51
55	122.68	9.01	122.89	9.03	139	123.58	7.36	124.36	7.36
64	116.96	8.91	117.03	8.92	142	111.72	8.25	111.72	8.25
65	124.19	8.62	124.42	8.63	144	114.74	8.44	114.92	8.50
66	128.59	9.50	nd[a]	nd[a]	145	112.58	8.68	112.68	8.69
71	112.17	8.56	112.08	8.51	146	124.92	8.81	125.04	8.86
73	126.82	8.49	127.05	8.47	147	119.49	7.93	119.58	7.94
74	116.73	8.26	nd[a]	nd[a]	148	119.01	8.66	119.31	8.63
75	126.82	8.57	nd[a]	nd[a]	150	124.95	7.67	125.00	7.70
76	115.58	8.92	115.89	8.92	151	117.87	8.86	118.11	8.85
78	120.77	7.81	120.91	7.81	153	105.82	7.48	105.25	7.42
80	119.30	8.04	119.31	8.04	154	122.18	7.06	122.20	7.06
85	nd[a]	nd[a]	133.39	10.59	156	122.01	7.81	122.02	7.81
87	105.13	7.46	104.78	7.41	157	119.47	7.60	120.61	7.63
88	122.65	8.59	122.97	8.64	158	115.40	7.59	nd[a]	nd[a]
89	127.54	9.27	127.21	9.25	159	108.18	7.83	108.24	7.84
90	125.04	9.30	125.11	9.27	160	118.58	7.23	118.53	7.23
161	113.68	8.42	113.49	8.42	171	118.71	7.60	119.17	7.64
162	111.12	9.22	111.13	9.23	173	105.16	7.75	104.58	7.71
163	118.52	8.31	118.01	8.35	174	125.43	7.36	125.41	7.36
164	120.28	7.92	120.21	7.93	175	118.30	7.76	118.30	7.76
165	111.60	8.35	111.60	8.35	176	111.47	8.26	111.49	8.25
166	118.34	7.86	118.38	7.86	177	119.33	7.85	119.34	7.85
167	116.70	8.84	116.80	8.86	178	124.42	8.32	124.39	8.31
168	121.04	7.90	121.01	7.89	179	131.24	7.98	131.28	7.97
170	125.47	9.18	125.40	9.18					

[a] nd: not determined.

ten of them located on loops L1 and L2 and five on the S51−T60 and G95−S107 fragments. The remaining residues belong to the flanking regions except Q124 and D129 which are on a loop close to loop L2.

The holoHasA−HasR Complex. The CRINEPT−TROSY spectrum of holoHasA in the holoHasA−HasR complex appears very different from that of free holoHasA, as observed from the superimposition of the two spectra reported in Figure 4B. From the comparison of the CRINEPT−TROSY spectra of the complexes (Figure 4C), it is apparent that the spectrum of holoHasA−HasR is superimposable with that of apoHasA−HasR. Therefore, in the complexes, holo- and apoHasA share the same spectral fingerprint, and the assignments obtained for the CRINEPT−TROSY of apoHasA−HasR could be easily transferred to the spectrum of holoHasA−HasR, with maximum chemical shift differences between corresponding resonances smaller than or equal to 0.2 ppm. The obtained assignments are reported in Table 1.

As in the case of the apoprotein, the signals of holoHasA can be grouped in three different classes according to their behavior upon complex formation (Table S2, Supporting Information). Fifty-nine signals could not be identified and are reported in blue in Figures 5C and 5D. Eighty-six signals are only little affected by complex formation (chemical shift variations <0.50 ppm) and therefore correspond to resonances that do not change significantly their chemical environment going from the isolated holo to the holoHasA−HasR complex. Signals of thirty-three residues, colored in red in Figures 5C and 5D, clearly disappear from their original position in the isolated holoHasA. Sixteen of these resonances (W23, G28, D29, V30, V37, G47, G52, A56, N62, A69, N72, A82, Y86, D96, S107, and D129) coincide with those experiencing chemical shift changes in apoHasA upon binding to HasR. When not coincident, they belong to the regions found to be involved in the interaction in the apoHasA−HasR complex: G35 on loop L1; F78 on loop L2; I57, T60, G97, G100, G101, and T103 on the S51−T60 and G95−S107 fragments; T26, G44, F45, S49, V64, A66, F67, L85, and I108 on the flanking regions (Figure 5D). Therefore, the same protein areas are involved in the interaction with the receptor for both holo and apoHasA (Figures 5A and 5C).

Discussion

Spectral Profiling and Structural Implications. In the $^{1}H-^{15}N$ TROSY-HSQC spectra of isolated apoHasA and holoHasA there are important differences in chemical shift patterns (Figure 4D), that have been shown to reflect the structural differences between the two protein forms, the "open"conformation of the apo protein and the "closed" conformation of the holo protein.[5] In addition, the presence of the paramagnetic heme iron(III) center in holoHasA causes hyperfine contributions to the chemical shifts and the broadening beyond detection of 15 signals, i.e., the amide resonances of H32, T33, N34, N41, S42, L50, T60, T74, Y75, T76, L77, F78, H83, T84, L85.[7]

From a visual inspection, it appears that the differences observed for the isolated proteins (Figure 4D) are quenched upon complex formation (Figure 4C). Usually, NMR spectroscopists quantitate differences between $^{1}H-^{15}N$ maps obtained under different conditions using chemical shift mapping and Garrett plots.[20,21,25] In the present case, such an analysis is limited by the inability to assign several resonances in the complexed form of the protein. As the assignment is not available for many peaks in the spectra of the complexes, we have decided to measure the distance between the spectra using a statistical approach that is independent of peak identification but only relies on the analysis of spectral profiles. Such an approach is commonly used in the analysis of metabolic NMR profiles.[26] It is based on the comparison of spectral patterns regardless on the origin of similarities and differences. The number provided by the normalized distance matrix (and reported in Figure 6) are purely the results of the statistical spectral comparison.

The aim of this approach is to ascertain whether the spectral patterns of the different protein forms, i.e., apoHasA, holoHasA, apoaHasA−HasR, holoHasA−HasR, carry unique features that are conformation specific. The results are summarized in Figure

(25) Zuiderweg, E. R. *Biochemistry* **2002**, *41*, 1–7.
(26) Assfalg, M.; Bertini, I.; Colangiuli, D.; Luchinat, C.; Schafer, H.; Schutz, B.; Spraul, M. *Proc. Natl. Acad. Sci. U.S.A.* **2008**, *105*, 1420–4.

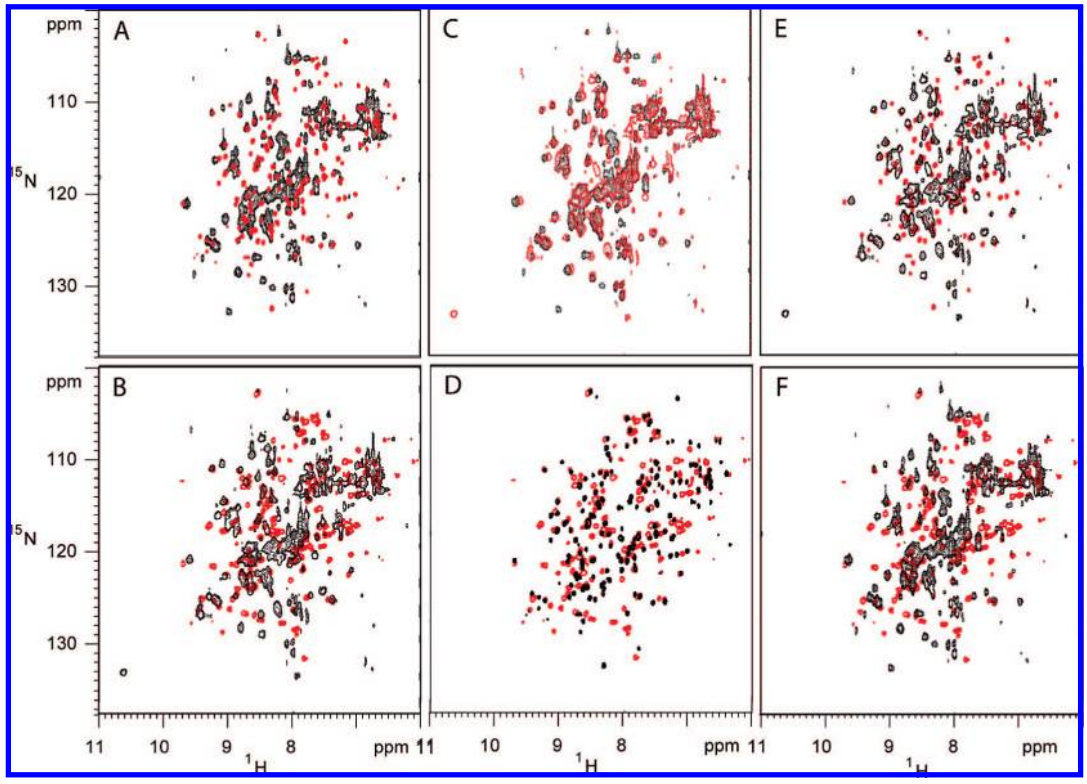

Figure 4. Superimposition of the spectra of (A) apoHasA (red) with apoHasA−HasR (black), (B) holoHasA (red) with holoHasA−HasR (black), (C) apoHasA−HasR (black) with holoHasA−HasR (red), (D) apoHasA (black) with holoHasA (red), (E) apoHasA (red) with holoHasA−HasR (black), and (F) holoHasA (red) with apoHasA−HasR (black).

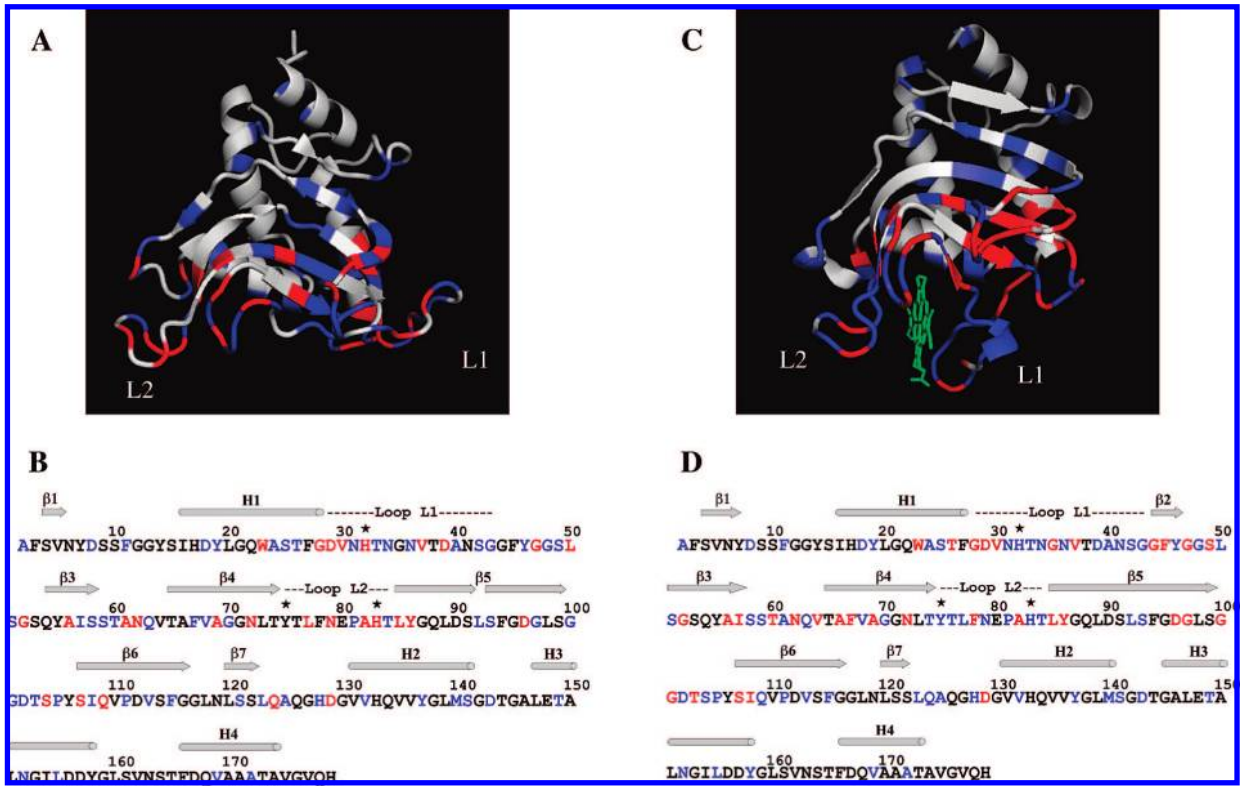

Figure 5. Overall 3D tertiary structure of apoHasA (PDB id 1YBJ) (A) with primary and secondary structures (B). Overall 3D tertiary structure of holoHasA (PDB id 1B2V) (C) with primary and secondary structures (D). Residues not affected when binding to HasR (class 1) are in gray, residues severely affected (class 2) are in red, residues not safely defined are in blue. Heme is in green. The two iron axial ligands (H32 and Y75) and residue H83 are labeled with a star in panels B and D.

6, where the numbers are a measure, arising from the statistical analysis, of the distance between pairs of spectra. In the reported scale a value of zero corresponds to identity, while an index of 1 is attributed to the pair resulting in the largest difference. In

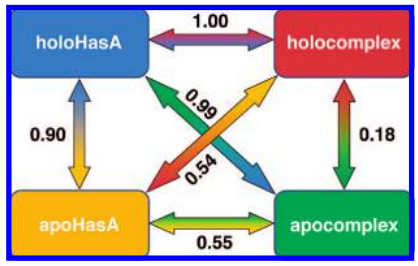

Figure 6. Schematic representation of the results obtained from the statistical analysis of the spectral profiles for apoHasA, holoHasA, apoHasA−HasR, and holoHasA−HasR. Numbers reported on each arrow are the values of the normalized distance matrix obtained for each pair of spectra.

Table 2. Comparison of the ^{1}H and ^{15}N Chemical Shift Values (ppm) for the Backbone Amides of Residues G35, T76, and F78 in the Four Protein Species: apoHasA, holoHasA, apoHasA−HasR, holoHasA−HasR[a]

	ApoHasA	holoHasA	ApoHasA−HasR	HoloHasA−HasR
G35	8.81	9.74	8.83	8.86
	113.93	112.47	114.06	113.44
T76	9.02	nd[b]	8.92	8.92
	115.98	nd[b]	115.58	115.89
F78	7.82	6.59	7.81	7.81
	120.83	120.01	120.77	120.91

[a] Shifts have been measured in 20 mM phosphate, pH 7 and 5 mM 2H DPC at 303 K. [b] nd: signal is not detectable because of its large line width induced by the closed proximity to the paramagnetic center.[7]

this frame holoHasA and apoHasA spectra (Figure 4D) are quite distant (0.90), while apoHasA−HasR and holoHasA−HasR (Figue 4 C) are very close (0.18). The comparison of spectra of samples of different molecular size must be handled with more care because of the different line widths. However, the relative values of distance indexes are informative. Indexes of 0.55 and 0.54 are obtained for apoHasA compared with apo-complex (Figure 4A) and holo-complex (Figure 4E), respectively. Indexes of 0.99 and 1.00 are obtained for holoHasA compared with apo-complex (Figure 4F) and holo-complex (Figure 4B), respectively. In summary, signal patterns are similar between apoHasA and apoHasA−HasR on one side, between apoHasA and holoHasA−HasR on the other side, and between the two complexes but always different from the pattern of the isolated holo form. This analysis provides a quantitative demonstration that, independently of the assignment, the two complexes have the same spectral signature, and that the spectral features of the isolated apoHasA are much closer to those of the complex than those of the isolated holoHasA.

We therefore demonstrate the existence of a conformational fingerprint and show that it constitutes a strong characteristic of each protein form as to allow its identification from the analysis of the spectral pattern. The clear outcome from the statistical analysis is that only three conformations are accessible to HasA in solution: that of the isolated holoprotein, that of the isolated apoprotein, and the conformation in the complex.

Monitoring Heme Binding via Paramagnetic Effects. The similarity between the CRINEPT−TROSY spectra of apoHasA−HasR and holoHasA−HasR holds also for resonances that were strongly affected by paramagnetic effects in free holoHasA. This is the case, in particular, of T76 and F78 on loop L2, and G35 on loop L1, as summarized in Table 2. T76 resonance was undetectable in the $^{1}H-^{15}N$ HSQC spectra of isolated holoHasA because of severe line broadening resulting from its proximity to the paramagnetic iron(III) center but reappears in the spectrum of holoHasA−HasR at the same shift as in the spectra of apoHasA−HasR and free apoHasA and with a line width that, within the experimental error, is the same as in the apoHasA−HasR spectrum. Signals of F78 and G35 have been reported[7] to experience hyperfine shift contributions, that have been evaluated by subtracting from the observed shift in holoHasA the shift of the corresponding gallium(III)−protoporphyrin HasA, taken as a diamagnetic reference of the holoform of HasA, with which it shares the closed conformation.[27] The signal of F78 in isolated holoHasA has hyperfine shift contributions of −0.58 ppm for ^{1}H and −0.56 ppm for ^{15}N.[7] In the CRINEPT−TROSY spectrum of holoHasA−HasR, it has the same shift as in the apoHasA−HasR spectrum with values typical of free apoHasA. Likewise, G35, characterized by hyperfine shift values of 0.51 ppm for ^{1}H and 0.36 ppm in free holoHasA[7] changes its shift upon complexation to HasR to values similar to apoHasA−HasR and typical of the apo protein.

In the gallium(III)−protoporphyrin HasA, the chemical shift values of G35, T76, and F78 are largely different from those of apoHasA, because of existing differences in the structures of the two proteins ($\Delta\delta_{tot}$ = 0.774, 1.523, and 0.575 respectively).[5] Therefore, the similarity in shifts with the apo and the differences in shifts with the gallium−protein for these signals further confirm that in the holoHasA−HasR complex, HasA has the typical shifts of the open conformation apo form.

An important conclusion that can be drawn from the behavior of residues that were considered paramagnetic in the isolated holoHasA is that the large paramagnetic effects due to the heme iron(III) characteristic of holoHasA are no longer present in the holoHasA−HasR complex.

Spectroscopic studies have shown a change in heme axial coordination in the holoHasA−HasR complex, and this behavior has been interpreted in terms of heme translocation from HasA to HasR.[10] After submission of this manuscript, the structure of the complex was solved (unpublished data), which confirms the above finding. The quench of paramagnetic effects in the spectra of holoHasA−HasR is consistent with this picture.

Further evidence would have been the identification in the holoHasA−HasR complex of resonances arising from the key active site residues, H32, Y75, and H83. These signals were undetectable in the spectra of free holoHasA. H32 and H83 fall in crowded regions of the free apoHasA spectrum and therefore could not be identified in the CRINEPT−TROSY spectrum of apoHaA−HasR. Concerning Y75, its signal in the apoHasA−HasR spectrum is clearly observed, but an obvious corresponding signal could not be detected in the spectrum of holoHasA−HasR. A possible candidate is a broad peak, at 8.22 and 126.5 ppm in the spectrum of holoHasA−HasR, that is not present in apoHasA−HasR (indicated by a red star in Figure 3B). In a further effort to identify Y75 in the holoHasA−HasR complex we acquired $^{13}C-^{13}C$ NOESY. Indeed, the ^{13}C-direct detection approach has proven to be useful in providing Cβ−Cγ correlations for Y75 in a HasA form where this residue was removed from heme iron(III) axial coordination.[28] Unfortunately, the combination of large molecular weight and relatively low concentration of the complex (ca. 0.3 mM) prevented detection

(27) Deniau, C.; Couprie, J.; Simenel, C.; Kumar, V.; Stojiljkovic, I.; Wandersman, C.; Delepierre, M.; Lecroisey, A. *J. Biomol. NMR* **2001**, *21*, 189–90.
(28) Caillet-Saguy, C.; Turano, P.; Piccioli, M.; Lukat-Rodgers, G. S.; Czjzek, M.; Guigliarelli, B.; Izadi-Pruneyre, N.; Rodgers, K. R.; Delepierre, M.; Lecroisey, A. *J. Biol. Chem.* **2008**, *283*, 5960–70.

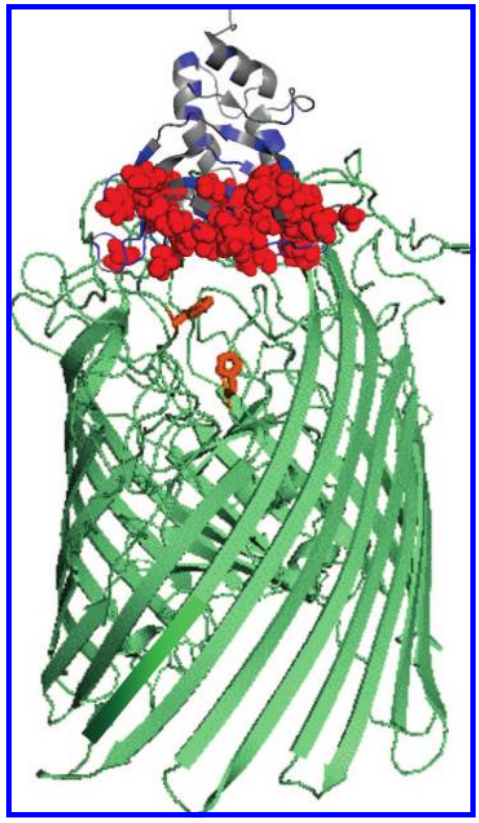

Figure 7. Representation of the HasA−HasR complex. Relative positioning of the HasA on HasR is purely schematic. The reference structure for HasA is that of free apoHasA (PDB id 1YBJ) which, on the basis of our spectral profiling, is the closest to that of HasA bound to HasR. The same color code as in Figure 5 is used. Residues shown as red spacefill correspond to those identified as belonging to the interaction surface. HasR, here represented by the available 3D model,[8] is in green with the two proposed axial histidine ligands in orange.

of aromatic Cβ−Cγ signals with enough resolution and signal-to-noise in the case of both apoHasA−HasR and holoHasA−HasR complexes. However, the aliphatic part of both spectra are almost superimposable (Figure S1, Supporting Information), thus indicating that the two complexes share a very similar, if not identical, side-chain orientation.

Different positions for the Y75 resonance in the apo-complex and holo-complex together with the disappearance of a few peaks of holoHasA, boxed in Figure 3A, may be ascribed to the paramagnetic contribution of the heme bound to the receptor. In HasR, two histidines conserved (H189 and H603) in the other heme/hemoprotein receptors have been shown to be involved in heme binding and heme transfer from HasA to HasR. Our data are in agreement with the structure of the complex[8,9] that shows that these two residues are indeed located at the surface of the receptor (Figure 7).

The heme transfer from holoHasA to HasR and binding to two His residues implies changes in the heme iron(III) coordination environment and spin state. Unfortunately, the ^{1}H-heme resonances in the complex are broadened beyond detection due to Curie effects[29,30] that are operative at high magnetic fields for a complex of this size (the heme is not ^{13}C labeled), and therefore we could not directly monitor changes in heme spins state and/or axial coordination.

Concluding Remarks

The above results represent the first description of the structural features of the complex formed between the hemophore HasA and its outer membrane receptor HasR in solution. The CRINEPT−TROSY fingerprints of holoHasA−HasR and apoHasA−HasR are the same, demonstrating a unique conformation for the hemophore in both complexes. Only three possible conformations for HasA are detectable in solution: a closed conformation for the isolated and metalated protein, an open conformation for the isolated apo protein, and the conformation in the complex. The statistical analysis of the NMR spectra indicates that the conformation in the complex is heme independent and similar to the open conformation of the isolated apo protein.

The protein−protein interaction occurs over a large surface area of HasA which involves the heme binding pocket, in particular loops L1 and L2, and part of the β face. The surface area is the same in the presence and in the absence of the heme.

In the complex obtained upon interaction between holo-HasA and HasR, the heme is transferred on HasR. The available biological information indicates that the heme transfer from HasA to HasR is energy independent whereas the translocation of the heme toward the periplasm and the release of HasA from HasR are energy-dependent processes controlled by the HasB−ExB−ExbD complex.[10,31] Our data confirms that heme transfer only requires the complex formation between HasA and HasR. The affinity for heme is higher for free HasA ($K_a = 5.5 \times 10^{10}$ M^{-1}) than for free HasR ($K_a = 5 \times 10^{6}$ M^{-1}), but the fact that complete heme transfer from holoHasA to HasR occurs in the in vitro complex implies that the observed conformational changes in HasA when bound to HasR are able to invert the order of relative affinity.[10] It has been reported that modulation in the H-bond network involving the axial ligand Y75 are sufficient to affect its ability to bind the iron and therefore to reduce the affinity of HasA toward the heme moiety.[28] The present chemical shift data indicate that in holoHasA complexed to HasR loop L2 assumes a conformation that resembles that of apoHasA, but different from that of the gallium(III)−protoporphyrin protein, and therefore consistent with the loss of the Y75 ligand. In addition, loop L1, containing the H32 axial ligand undergoes structural rearrangements consistent with the open structure of apoHasA. Noteworthy, such a loop could not be modeled because of missing electron density in the X-ray structure of the complexes,[9] and therefore our NMR data complement the crystal structure information. Reasonably, these structural changes are at the basis of a decreased affinity for heme, so that in the complex it can be transferred to the HasR receptor.

For functional purposes, the interaction between the hemophore and the receptor has to be transient. However, in DPC micelles a stable complex is detected. The consideration that in vivo heme internalization through the receptor and release of the apo hemophore HasA requires energy provided by HasB and related proteins, i.e., by macromolecular

(29) Gueron, M. *J. Magn. Reson.* **1975**, *19*, 58–66.
(30) Vega, A.; Fiat, D. *Mol. Phys.* **1976**, *31*, 347–355.
(31) Lefevre, J.; Delepelaire, P.; Delepierre, M.; Izadi-Pruneyre, N. *J. Mol. Biol.* **2008**, *378*, 838–49.

components that are not present in vitro, can solve this apparent contradiction.

Acknowledgment. We thank C. Wandersman and P. Delepelaire for helpful discussion. NMR experiments were run at the EUNMR Research Infrastructure (contract no. RII3-026145, EU-NMR). PRIN 2005, MIUR FIRB - RBIP06LSS2, and the Caisse nationale du RSI are acknowledged for financial support.

Supporting Information Available: Assignment tables and chemical shift variations upon complex formation. Aliphatic part of the $^{13}C-^{13}C$ NOESY of apoHasA−HasR and holo-HasA−HasR. This material is available free of charge via the Internet at http://pubs.acs.org.

JA804783X